CoNF-961202--75   ANL/CMT/CP--90406

SOLUTION-BORNE COLLOIDS FROM DRIP TESTS USING ACTINIDE-DOPED AND FULLY-RADIOACTIVE WASTE GLASSES

RECEIVED
FEB 20 1997
OSTI

Jeffrey A. Fortner, Stephen F. Wolf, Edgar C. Buck, Carol J. Mertz, and John K. Bates

Chemical Technology Division
ARGONNE NATIONAL LABORATORY
9700 South Cass Avenue
Argonne, IL 60439-4837

MASTER

Submitted to

1996 Fall Meeting
Materials Research Society
Boston, MA
December 2-5, 1996

DISTRIBUTION OF THIS DOCUMENT IS UNLIMITED

DISCLAIMER

SOLUTION-BORNE COLLOIDS FROM DRIP TESTS USING ACTINIDE-DOPED AND FULLY-RADIOACTIVE WASTE GLASSES

Jeffrey A. Fortner, Stephen F. Wolf, Edgar C. Buck, Carol J. Mertz, and John K. Bates.
Argonne National Laboratory, Argonne, IL 60439, USA.

ABSTRACT

Drip tests designed to replicate the synergistic interactions between waste glass, repository groundwater, water vapor, and sensitized 304L stainless steel in the potential Yucca Mountain Repository have been ongoing in our laboratory for over ten years. Results will be presented from three sets of these drip tests: two with actinide-doped glasses, and one with a fully-radioactive glass. Periodic sampling of these tests have revealed trends in actinide release behavior that are consistent with their entrainment in colloidal material when as-cast glass is reacted. Results from vapor hydrated glass show that initially the actinides are completely dissolved in solution, but as the reaction proceeds, the actinides become suspended in solution. Sequential filtering and alpha spectroscopy of colloid-bearing leachate solutions indicate that more than 80% of the plutonium and americium are bound to particles that are captured by a 0.1 µm filter, while less than 10% of the neptunium is stopped by a 0.1 µm filter. Analytical transmission electron microscopy has been used to examine particles from leachate solutions and to identify several actinide-bearing phases which are responsible for the majority of actinide release during glass corrosion.

INTRODUCTION

Drip tests designed to simulate potential conditions in the proposed Yucca Mountain Repository have been in progress with both actinide-doped and fully radioactive glasses. These tests react slowly dripping, tuff-equilibrated groundwater with a monolithic waste glass sample, sensitized 304L stainless steel, and water vapor to determine synergistic interactions possible in a compromised pour canister under unsaturated conditions. The tests using actinide-doped Savannah River Laboratory (SRL) 165 glass, termed the N2 test series, have been ongoing for over 10 years. Tests with a West Valley Demonstration Project former reference glass (ATM-10) have been in progress for 8 years and are termed the N3 test series. A modified drip test with a radioactive sludge-based SRL 200R glass that had been pre-aged, along with its 304L stainless steel holder, in 200°C water vapor has been termed the N4 test series, and has been ongoing for nearly 5 years. During this time, the release of actinides and fission products to solution has been measure d[1-4], and the role of solution-borne colloids in this release has been explored as presented below.

While it has been established that radioactive waste glass can release radionuclides via colloids [1,5], details of the long-term role of colloids in the source term from glass corrosion have not been well documented. Clearly, radionuclides can be sorbed from solution onto aboriginal groundwater colloids (pseudocolloids) or become incorporated into colloidal material that nucleates from dissolved species in solution (radiocolloids). Each of these colloid formation mechanisms would be limited in their potential for transport by the solubility of the radionuclides, and thus are unlikely to substantially increase the release of these elements from the waste package environment. However, as glass reacts it alters to clay and other mineral phases which may spall from the surface, often as colloid-sized particles. This third type, termed primary colloids, can release radionuclides at levels bounded only by the reaction rate of the source glass.

When solution conditions become unstable for colloids, the colloids will flocculate and sediment, attaching themselves either to the test vessel or to the surface of the glass [6]. In the case of drip tests, the low flow results in particles dislodging from the reacted surface. Alternatively, if the ionic strength of the passing water is low, or if the pH is high, alteration phases may be dislodged through increasing particle-particle repulsive forces [6]. At Yucca Mountain, migration may be enhanced if the surface of the fractures in the tuff possess a similar surface electrical potential to the clay colloids, whereas other types of waste-glass-derived colloids may be retarded if the surface charges are different. Therefore, it is important to know the physical properties of the colloids generated due to waste glass reaction. Pseudocolloids and radiocolloids, which can

only marginally increase transport above the solubility limits, may serve to decrease net release by sweeping radionuclides from solution and later plating out onto nearby host rock in the repository. Primary colloids may allow rapid release of radionuclides above solubility limits, which is particularly important for the release behavior of glass. In our laboratory tests, the glasses release nearly all of the long-lived radionuclide content (except neptunium) in the form of colloids. In the experimental work discussed in this paper, we address preliminary efforts to address the formation and characterization of the colloidal material formed in the very near-field, and do not address the potential for the observed species to migrate from the proposed repository. More detailed information regarding the characterization of colloids is required to complete the performance assessment of the repository.

EXPERIMENTAL

Unsaturated (Drip) Test Method

The drip tests, which follow the Unsaturated Test Method, are described in detail elsewhere [2,3], but will be described briefly in order to define a context for the data. The Unsaturated Test Method simulates the potential repository conditions where glass, stainless steel, and water (liquid and vapor) interact. Test parameters can be adjusted to reflect changes in water chemistry and flow rate that may occur.

Each ongoing test series consists of 3 identically-prepared samples and a blank. Every 3.5 days, approximately 3 drops (0.075 mL) of conditioned groundwater from the J-13 well (EJ-13 water) is injected into the airtight vessel where it contacts the top surface of the waste package assemblage (WPA). The WPA consists of a glass monolith contacted on the top and bottom by two perforated retainer plates made from sensitized 304L stainless steel, which are held in place by two wire posts, also made from 304L stainless steel. The entire apparatus is enclosed in a 90°C oven except when samples are taken. Water drips down the sides of the glass and accumulates at the bottom of the WPA. Eventually the water drips from the WPA to the bottom of the test vessel. When tests are sampled (currently at 26-week intervals) the WPA is examined visually to qualitatively ascertain the degree of reaction, including evidence of alteration phase formation and possible spalling of the alteration phases and clay layer. After observation, the WPA is transferred to a fresh test vessel, the test solution removed for analysis, and the just-used vessel is acid-stripped to determine sorbed species.

Analytical Radiochemistry

The sampled solutions from the bottom of the test vessel are analyzed using inductively-coupled plasma mass spectrometry (ICP/MS) plus high-resolution alpha and gamma spectrometry. When sufficient solution is collected, sequential filtering is performed with filters of 1 μm and smaller. Recently, solution has been filtered through a Millipore MC® filter in an ultracentrifuge. The filtered solutions from each test series typically have more than ~80% of the Am and Pu removed by a 0.1 μm filter. The ultracentrifuged filtered samples have had nearly 100% of the Am and Pu removed, with full recovery (no removal) of the Np.

As the glass reacts, material is released from the glass either truly dissolved in solution or as particulate material. The solution is also in contact with the pre-sensitized 304L stainless steel retainer during the reaction process, so the analysis of the solution collected in the bottom of the test vessel represents all the material that is transported from the glass and glass retainer. The solution is analyzed for its constituent parts as described above, but all the material analyzed in the test solution is considered to have been released from the glass/stainless steel assembly.

Analytical Transmission Electron Microscopy

A 5 μL aliquot is prepared for analytical transmission electron microscopy (AEM) by wicking the unfiltered solution through a "holey" (perforated) carbon sample grid. The AEM is carried out with a JEOL 2000FX II transmission electron microscope equipped with two Noran energy dispersive X-ray fluorescence (EDS) detectors (one at high-angle and the other having an

ultra-thin window), plus a Gatan model 666 parallel electron energy loss spectrometer (EELS). Identification of crystalline materials with AEM is often possible using electron diffraction. However, the radionuclide content of the colloids and general physical characteristics, e.g., size distribution and charge, cannot be determined with AEM. Additionally, the colloids identified are representative only of the material in the 5 μL sample.

Dynamic Light Scattering

Dynamic light scattering (DLS) is used to probe the dynamics of microscopic particle motion. The principles governing the application of light scattering to study many systems is described elsewhere [7,8]. The technique is used to determine the size and distribution of colloidal-sized particles in the range of one or two nm to several μm. This technique is based on the measurement of fluctuations in scattered light intensity caused by the Brownian motion of the particles in solution. Time scale fluctuations in light intensity are measured as individual scattered photons into time windows that span a range of the scattering signal. The measured autocorrelation function of these data is fit by well-accepted methods to determine the particle size distribution [9-11].

The scattering experiments were carried out on a modified 4700C Photon Correlation Spectrometer from Malvern Instruments, Ltd. The particle sizing data analysis was done using standard methods [7,9]. Light scattering measurements were made on solution extracted from the N4 tests since measurements are taken immediately upon sampling and at time periods thereafter. These tests were just recently sampled, during the development of the DLS method. Laser light scattering system calibration was performed with a series of NIST traceable polystyrene (PS) latex standards (32, 73, and 304 nm) from Duke Scientific Corp. Standard solutions were sampled in filtered deionized water according to certification instructions. The PS data were fit by cumulants and were in excellent agreement with the certified standards. The EJ-13 water contained no DLS-measurable colloids prior to interacting with glass in a test.

RESULTS AND DISCUSSION

An example of the apparent role of colloids in actinide release appears in Fig. 1. Here, the cumulative normalized release (from *unfiltered* test solution) of the elements B, Np, Pu, and Am from one of the three ongoing tests in the N2 series display a behavior that is best explained by a release of particulate material to solution. The soluble elements B and Np were initially released at a substantially greater rate than the relatively insoluble elements Pu and Am. At later times (after ~8 years), the spallation of alteration phases, some of which have incorporated Pu and Am, led to total release of these elements approaching that expected from congruent dissolution of the glass. Sequential filtering has confirmed that more than 80% of the Pu and Am, but very little of the Np, in solution from the N2 series are trapped by a 0.1 μm filter. Some of the potential actinide-bearing alteration phases have been observed using AEM. Many of these particles have small (<1 μm) linear dimensions and high surface areas characteristic of colloids. Examples of these particles, plus others from the N3 and N4 series, are described in detail below.

In both the N2 and N3 tests, the majority of colloidal particles observed by AEM have been either a smectite-type clay or a variety of iron-silicates (Fig. 2). Both clays and iron silicates can sorb actinides, and thus these colloids represent potential transport mechanisms for insoluble elements. As stated previously, more than 80% of the Pu and Am in solution from the N2 and N3 tests appears to be associated with particulate matter that will not pass through a 0.1 μm filter. In the N2 tests, both the clay and iron-silicate colloids are sometimes observed to contain small amounts of uranium. Uranium is also observed on occasion in the clays and iron-silicates from the N3 tests; thorium is generally detected only in an entrained alteration phase such as the thorium calcium orthophosphate mineral *brockite* [1,5,12], and not in the clay itself. Examples of brockite-containing colloids, including evidence for their high transuranic content, have been published elsewhere [1,5]. The aged 200R glass in the N4 drip tests also produced a brockite-like alteration phase rich in rare earth elements (Fig. 3). None of the above colloid particles were observed in wicked solution from the blank tests.
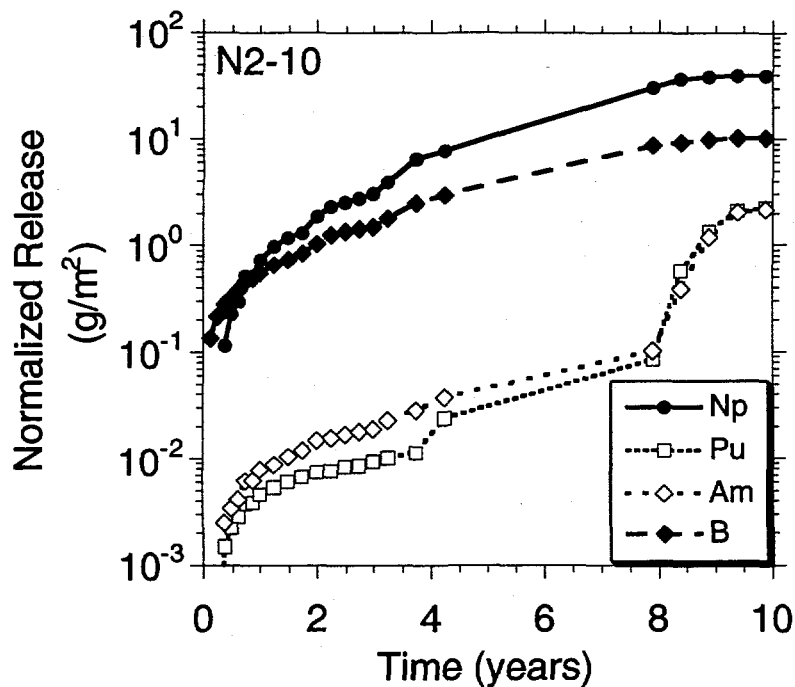
Fig. 1. The cumulative normalized release of the elements B, Np, Pu, and Am from one of the tests in the N2 series. The sudden increase in the release of the insoluble elements Pu and Am shortly after 400 weeks is strong evidence of the role of colloids in the release of these elements from the WPA. Almost no Am or Pu appears in filtered solution, while the Np in filtered solution is essentially the same as that in the unfiltered. The lines are a guide to the eye.

Sparingly soluble or insoluble elements that are not incorporated into the clay structure, or that are present at levels beyond what can be accommodated by clay, will precipitate as alteration phases on the reacted glass and nearby surfaces, such as the stainless steel retainer. As the solution composition evolves with time during glass and steel corrosion, so too will the assemblage of alteration phases evolve. The major constituents in the glass that are not completely dissolved into solution will be incorporated into the clay or will form distinct alteration phases (such as brockite). Excess iron is also present due to the corroding 304L stainless steel.

Once nucleated, the clay layer continues to grow and evolve. Growth occurs as the hydrated glass layer beneath the existing clay dissolves in a nearly congruent manner, and the elements from solution saturate and reprecipitate onto the surface of the clay. Voids are frequently observed between the clay and glass, a result of either disproportionate growth/dissolution rates or accumulating strain due to different materials properties between the glass and the clay layer. The etching of the glass beneath the clay continues in an irregular manner, leaving some points of contact between the clay and glass, holding the layer in place. This clay layer may spall away, however, as stress builds up in the structure and as the glass etches away beneath. This is likely the origin of the clay colloid particles observed in solution from the drip tests. Thus, as the clay becomes detached from the WPA, actinide-bearing alteration phases may be released. This results in the delayed release of Pu and Am as colloidally-suspended particles, as illustrated in the solution data of Fig. 1. However, the transuranic content of the specific phases (as in Figs. 2 and 3) cannot be determined with AEM, and this additional information is required to perform performance assessment calculations which include release from glass in the source term.

The source of primary colloids is the altered surface of the WPA. In order to confirm the characteristics of the source of these colloids, sections of the reacted surface plus alteration phases were removed from the N3-9 and N3-10 glass monolith surfaces during the July 1995 sampling of the N3 tests. These samples, measuring about 5 μm (or less) across, were imbedded in epoxy resin, thin-sectioned to approximately 50 nm thickness using a diamond-knife microtoming process, and placed on a transmission electron microscope grid for AEM examination.

The particles removed from the N3-9 surface were discrete alteration phases, while that removed from the N2-10 was a fragment of the spalling clay layer. The N3-9 particles were found to be an amorphous silica alteration phase, plus a variety of iron silicate and iron silicate hydroxide phases, some of which were identified by electron diffraction as *iron hydroxide* [nominally FeO(OH)], *ferripyrophyllite* [nominally $Fe_2Si_4O_{10}(OH)_2$], and *erlianite* [nominally $Fe_6Si_6O_{15}(OH)_8$]. The N3-10 clay particle turned out to be an interesting composite of smectite clay
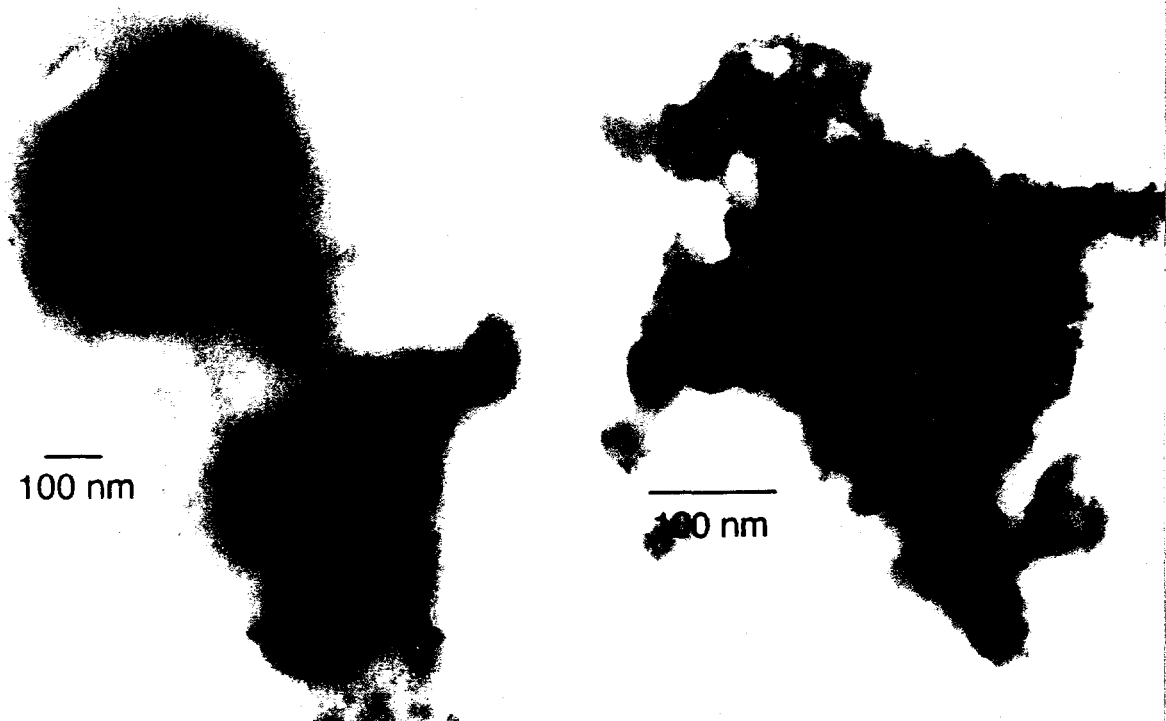
Fig. 2.   Typical AEM micrographs of colloid particles extracted from the drip tests. At left are 2 smectite clay colloid particles from the N2-12 Test sampled December 18, 1995. At right is an iron silicate colloid from the N3-9 Test sampled January 11, 1996.
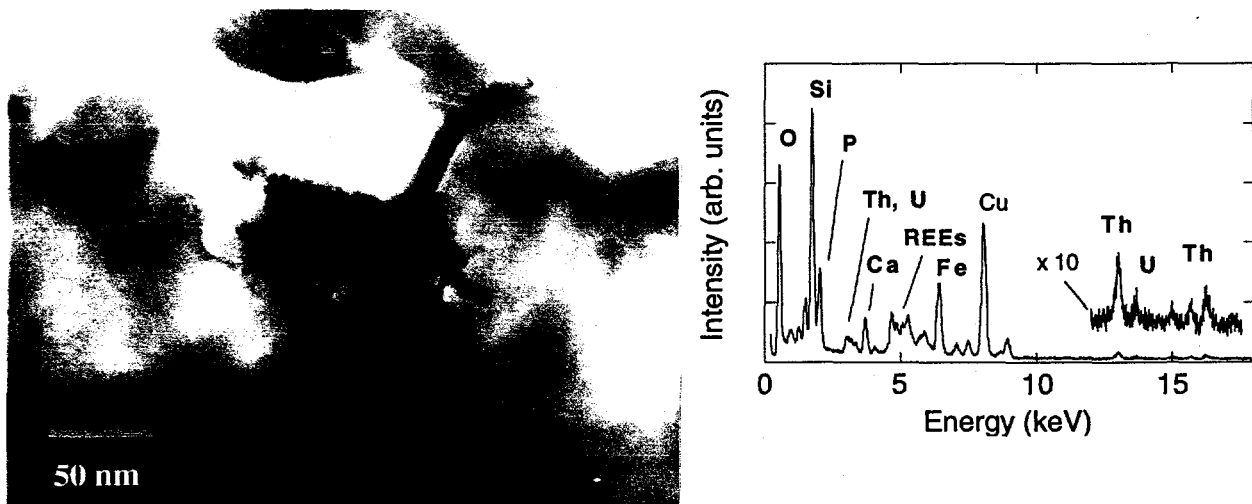

Fig. 3.   At left is a TEM image of a rare earth element (REE)-bearing phase from a 200R glass drip test (N4). The EDS analysis of the particle (right) demonstrates that it contains actinide elements.

with copious amounts of *brockite* (nominally, [Th, Ca, REE]PO_4), plus an amorphous thorium-titanium-iron silicate, similar to the mineral thorutite [nominally, (Th, U, Ca)Ti_2O_6]. A transmission electron micrograph of a portion of this N3-10 matrix material appears in Fig. 4. The chemical compositions of the individual phases are characterized by the EDS spectra of Fig. 5, while EELS analysis of REE and actinides in the brockite appears in Fig. 6. The distribution of rare earth and actinides is virtually identical to that observed in tests terminated after 1 year [12].
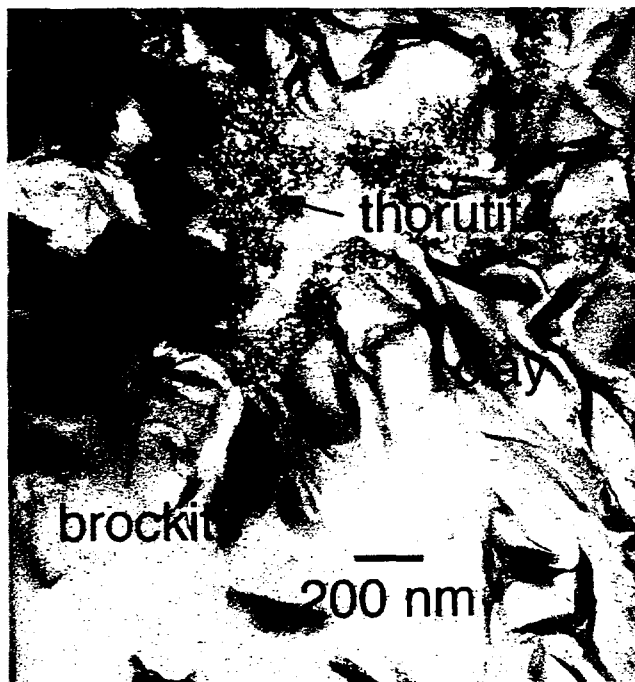
Fig. 4. The clay alteration layer on the N3-10 glass, sampled July 1995, was found to consist of a composite of smectite clay, brockite crystallites, and thorutite, as seen in this transmission electron micrograph. The thorutite forms in the solution between the layer and the dissolving glass and is trapped by the clay layer.

The dynamic light scattering measurements were made on a sample of test solution from the N4-2 test sampled in September 1996, after a 26-week test interval. The sample was held in a temperature-controlled water bath at 25°C during which measurements were made to monitor the stability of the colloids. Representative data from the correlator are shown in Fig. 7. The data indicated a broad distribution or polydisperse sample. Since the cumulants method is limited to narrow distributions with variances of 0.3 or less, the Contin program [9] was used for final data analysis and was able to resolve a bimodal distribution. In general, the largest suspended fraction (>95%) is attributed to a size fraction with a mean diameter of approximately 0.2 μm. A smaller fraction (<5%) with a mean diameter greater than 4 μm was also found suspended in all the samples. These size observations are consistent with both the filtration/alpha spectroscopy and the AEM data. The contribution from the larger size fraction reduced slightly during the ten day measurement period which can be attributed to settling of the larger particles.

The detection limits for the dynamic light scattering measurements were established using the PS standards. In general, particles that scatter light efficiently (e.g., good scattering contrast between the particle and the suspending medium) can be detected quite easily in the ppm concentration range. Particle sizing measurements can be made on concentrations of PS particles as low as 0.2 μg/g(solution). However, the detection limit of the instrument can be severely limited by the presence of dust and foreign material, as well as the scattering contrast of the particles, especially at sub-ppm concentrations. Efforts to quantify the method are ongoing.

CONCLUSIONS

Actinide-bearing colloids are formed during waste glass reaction under potential repository conditions. Candidate materials for actinide entrainment include smectite clay, iron silicates and iron silicate hydroxides. Some alteration phases can incorporate relatively large concentrations of actinides and rare earth elements and become mobilized as colloids when the surface clay is sloughed from the glass surface. The formation of stable, actinide-bearing alteration phases may be of benefit to the repository performance if transport is limited by the hydrology/geology of the site. The ability of these colloids to be transported through the waste package and the repository, and the range of their potential migration cannot be inferred from these tests, and will require separate consideration. However, input to performance assessment of colloidal transport must use a complete physical characterization of the primary colloids that may actually dominate the release of actinides from glass in a scenerio where the steel canisters are breached.

a

Counts — Energy (keV)

O, Si, Al, Fe, Cu

b

Counts — Energy (keV)

O, Si, P, Th, Ca, Nd, Fe, Cu, Th, U, Th

c
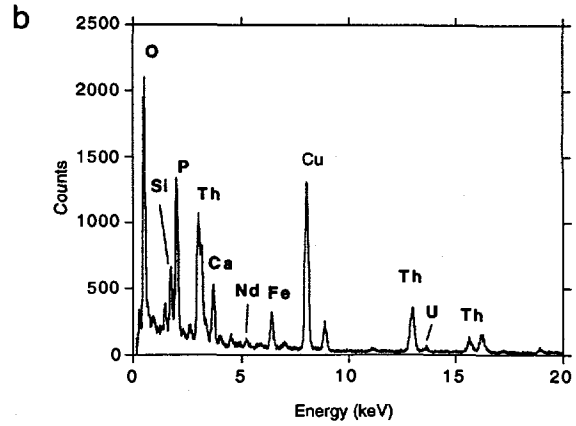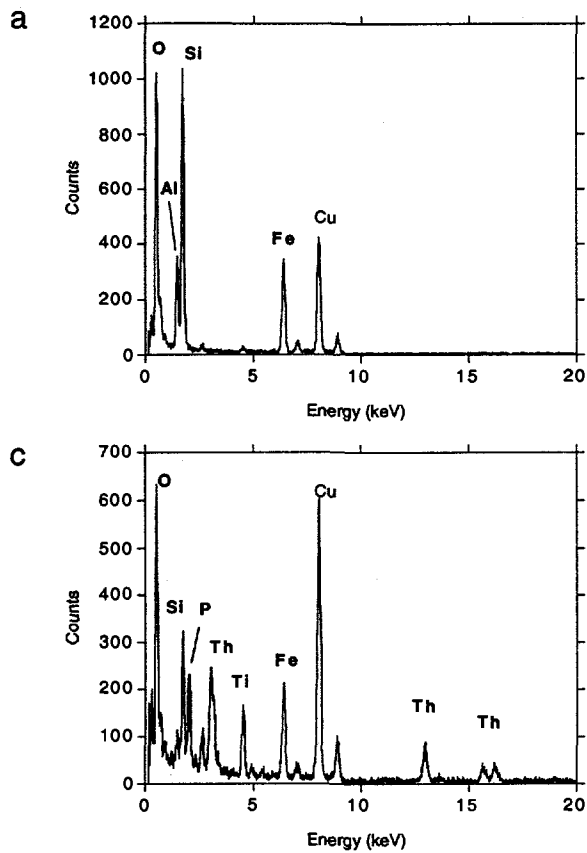
Counts — Energy (keV)

O, Si, P, Th, Ti, Fe, Cu, Th, Th

Fig. 5. The three components comprising the N3-10 clay composite were examined using EDS in the AEM, providing the above spectra of (a) smectite clay, (b) brockite, and (c) an amorphous Th-Fe-Si-Ti phase (similar to thorutite). The copper lines are an artifact of the sample mount. The EDS spectra of these phases accompany the labels in Fig. 4.

Second Difference Intensity (counts) — Energy Loss (eV)

Th-N$_5$, Th-N$_4$ & Fe-L$_{2,3}$, U-N$_5$, La-M$_4$, La-M$_5$, Ce-M$_5$, Ce-M$_4$, Nd-M$_5$, Nd-M$_4$, Ba-M$_5$, Ba-M$_4$
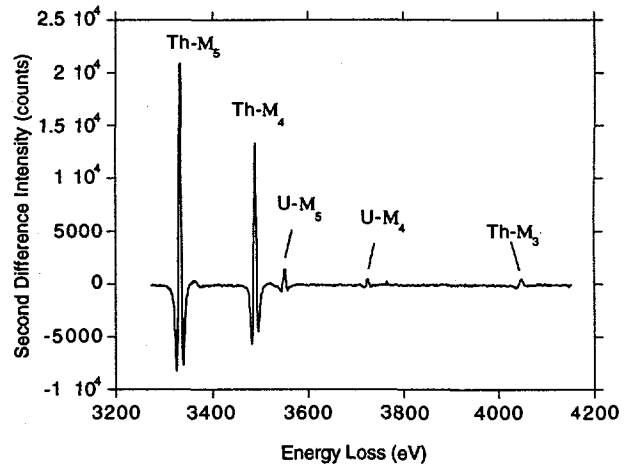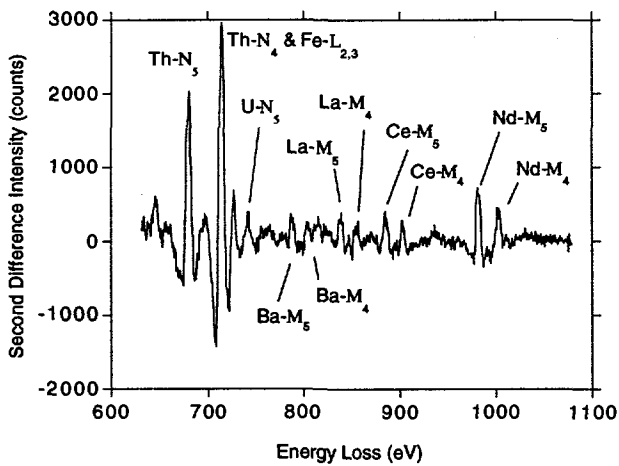
Th-M$_5$, Th-M$_4$, U-M$_5$, U-M$_4$, Th-M$_3$

Fig. 6.   The EELS spectra from the brockite indicate nearly identical distributions of REEs and actinides as that observed in brockite particles from tests terminated at times of one year or less [12].
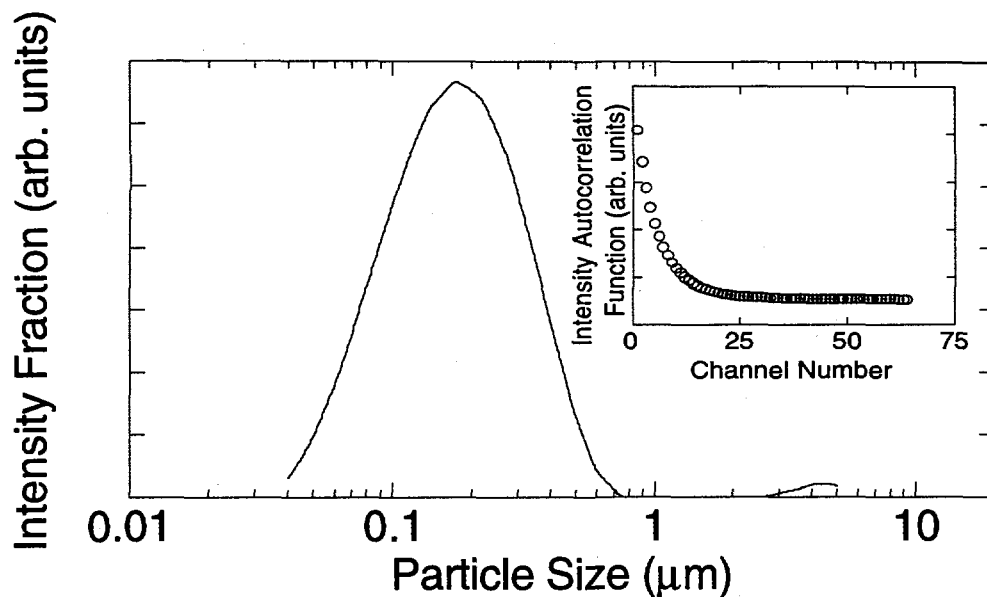
Fig. 7. Particle size distribution (from scattering intensity) with intensity autocorrelation function (inset) from the N4-2 test sampled September 1996. Note the bimodal distribution with peaks at ~0.2 and 4 μm.

ACKNOWLEDGMENTS

REFERENCES

1.   J. Fortner and J. K. Bates, *Mat. Res. Soc. Proc.* Vol. **412**, 205-211 (1996).
2.   J. K. Bates and T. J. Gerding, *One-Year Results of the NNWSI Unsaturated Test Procedure: SRL 165 Glass Application*, Argonne National Laboratory Report ANL-85-41 (1986).
3.   J. K. Bates and T. J. Gerding, *Application of the NNWSI Unsaturated Test Method to Actinide Doped SRL 165 Type Glass*, Argonne National Laboratory Report ANL-89/24 (1990).
4.   J. K. Bates and E. C. Buck, *Proceedings of the 1994 International High-Level Radioactive Waste Management Conference*, American Nuclear Society (1994).
5.   J. K. Bates, J. P. Bradley, A. Teetsov, C. R. Bradley, and M. Buchholtz ten Brink, *Science* **256**, 649 (1992).
6.   H. van Olphen, in *Clay Colloid Chemistry;* John Wiley & Sons, New York, 1977, pp. 92-108.
7.   B. Chu, *Laser Light Scattering*, 2nd ed., Academic Press, San Diego (1991).
8.   B. J. Berne and R. Pecora, *Dynamic Light Scattering*, John Wiley & Sons, Inc., New York (1976).
9.   S. W. Provencher, *CONTIN, User's Manual, Version 2*, EMBL-DA07, Euro. Molec. Biol. Lab., Heidelburg, Germany (March 1984).
10.   R. S. Stock and W. H. Ray, *J. Polymer Sci.: Polym. Phys. Ed.*, **23**, 1393 (1985).
11.   R. M. Johnsen and W. Brown, in *Laser Light Scattering in Biochemistry*, S. E. Harding, D. B. Satelle, and V. A. Bloomfield, Eds., Royal Society of Chemistry, Cambridge, 77 (1992).
12.   J. A. Fortner, T. J. Gerding, and J. K. Bates, in *Environmental Issues and Waste Management Technologies in the Ceramic and Nuclear Industries*, Ceramic Trans. Vol. **61**, V. Jain and R. Palmer, eds. pp. 455-462. (1995).